View metadata, citation and similar papers at core.ac.uk

brought to you by CORE

provided by Cork Open Research Archive

Title	Investigation of DMAB oxidation at a gold microelectrode in base
Author(s)	Rohan, James F.; Nagle, Lorraine C.
Publication date	2005-04-01
Original citation	Nagle, L. C. and Rohan, J. F. (2005) 'Investigation of DMAB Oxidation at a Gold Microelectrode in Base', Electrochemical and Solid-State Letters, 8(5), pp. C77-C80. doi:10.1149/1.1883905
Type of publication	Article (peer-reviewed)
Link to publisher's version	http://dx.doi.org/10.1149/1.1883905 Access to the full text of the published version may require a subscription.
Rights	**© 2005 The Electrochemical Society.**
Item downloaded from	http://hdl.handle.net/10468/3709

Downloaded on 2018-08-23T18:38:11Z

Investigation of dimethylamine borane oxidation at a gold microelectrode in base.

Lorraine C. Nagle and James F. Rohan*

NMRC, National University of Ireland, Cork, Lee Maltings, Prospect Row, Cork, Ireland.
* Corresponding author. Tel.: +353 21 4904224; fax: +353 21 4270271.
E-mail address: james.rohan@nmrc.ie (James F. Rohan)

Abstract

A gold microdisc has been used to determine the diffusion coefficient (D) for dimethylamine borane (DMAB) in concentrated alkaline solution. Two steady state oxidation waves are resolved through the use of microelectrodes. Using the D value determined, the coulomb number for both oxidation waves was shown to be 3. The first wave may be further resolved in dilute solutions revealing three 1-electron steps. The concentration range wherein the maximum coulombic efficiency for DMAB oxidation on gold may be achieved is demonstrated. An oxidation pathway with a variable coulomb number is suggested.

1. Introduction

Dimethylamine borane (DMAB), $(CH_3)_2NHBH_3$, is a technologically significant reducing agent for the electroless chemical deposition of metals [1-8], alloys [9-12], semiconductors [13,14] and most recently insulators [15]. Electroless deposition exhibits an advantage over electrodeposition in that deposition on insulators is possible following a catalytic activation of the substrate. In microelectronics applications the driver for the use of electroless plating baths has been the replacement of expensive vacuum metallisation methods with a low cost, low temperature, selective deposition method [16]. The practical use of DMAB as a reductant in electroless deposition has generated much interest in unraveling the mechanism of its oxidation [6,7,17]. To assist in plating bath formulation a thorough understanding of the reductant oxidation process is required [7,16]. Recently, a molecular orbital analysis has suggested a multi-step reaction proceeding via five-coordinate intermediates, $BH_x(OH)_y^-$ [6]. A coulomb number, n, of 3 was assigned to the overall process given in equation 1 where the oxidation number of boron changes from –3 to 3.

$$(CH_3)_2NHBH_3 + 4OH^- = B(OH)_4^- + (CH_3)_2NH + \frac{3}{2}H_2 + 3e^- \qquad [1]$$

Analysis of the adsorption-desorption behaviour of DMAB on Au substrates in base using coupled electrochemical quartz crystal microbalance and cyclic voltammetric techniques identified two transient borane-containing reactive intermediates during the irreversible oxidation of DMAB given by equation 2 [7]. The precise nature of the reactive intermediates was not established.

$$BH_3(OH)^- + 3OH^- = BO_2^- + \frac{3}{2}H_2 + 3e^- + 2H_2O \qquad [2]$$

In a cyclic voltammetric study of the oxidation behaviour of DMAB at a Au macroelectrode in base Burke et al. [17] emphasised the role of active Au cations and surface oxide layer in the overall oxidation of DMAB given by equation 3 which represents maximum coulombic efficiency for the oxidation reaction.

$$BH_3(OH)^- + 8OH^- = BO_3^{3-} + 6e^- + 6H_2O \qquad [3]$$

We describe here an investigation into the electrochemical oxidation pathway of DMAB at a Au microdisc in base to assist in the determination of the oxidation mechanism with a view to optimisation of electroless plating bath formulations and their operation. To date, critical information (namely n and D) has been absent in the analysis of DMAB oxidation. Bard et al. [18,19] demonstrated the application of microelectrodes in elucidating the multistage process of borohydride oxidation. A Au microdisc in base was used to directly determine D for borohydride and subsequently n with a value of 8 for its oxidation to borate inferred [18]. A study of this system using fast-scan cyclic voltammetry and scanning electrochemical microscopy distinguished at least two quasi-reversible stages in the oxidation pathway, the first of which was assigned a 2-electron transfer reaction [19]. Our approach seeks to exploit the unique properties of microelectrodes to further elucidate the mechanism of DMAB oxidation. The detection of subnanoamp current permits the analysis of dilute solutions. Furthermore, the virtual negation of charging current and Ohmic potential drop enables acquisition of undistorted voltammetric data. Our preliminary findings provide data for the further analysis of DMAB oxidation at Au in base.

2. Experimental.

Dimethylamine borane (minimum purity 97 %) and sodium hydroxide (minimum purity 99 %) were purchased from Sigma Aldrich and used as received. Deionised water of resistivity 18 MΩ cm was used to prepare all solutions. The working electrode was a 10 μm diameter Au microdisc (Princeton Applied Research) supplied by Advanced Measurement Technology, UK. This was polished with 0.5 μm alumina powder obtained from Struers on a Buehler polishing cloth for 1-2 minutes and rinsed in deionised water. A 0.5 mm diameter Pt electrode of 37 mm length (IJ Cambria) was used as counter electrode. A Ag/AgCl, KCl saturated electrode (IJ Cambria) was used as reference. The potential of the working electrode was controlled using a CH Instruments potentiostat model 620A. The effective cell volume was 20 ml. All solutions were purged with nitrogen for 20 minutes prior to experiments in order to remove oxygen. All experiments were performed at 20 ^{o}C.

3. Results and Discussion.

Au in base is the choice system for voltammetric investigation [7,17] of the oxidation pathway for DMAB. The virtual absence of a hydrogen adsorption region and negligible background current at Au in the potential region corresponding to DMAB oxidation permits analysis of low concentrations of DMAB. The oxidation at gold electrodes has been reported to involve electron loss of between 2 and 6 coupled to possible abstraction of the component hydrogen atoms. [6,7,17] In highly alkaline solution it is expected that DMAB will exist as the hydroxytrihydroborate ion,

$BH_3(OH)^-$, [3,7,17] which may undergo oxidation with maximum coulombic efficiency on Au in base according to the reaction,

$$BH_3(OH)^- + 6OH^- = B(OH)_4^- + 3H_2O + 6e^- \quad [4]$$

Competing chemical hydrolysis of DMAB with evolution of hydrogen, given by equation 5, is expected to be minimal at pH values in excess of 12 [18, 20].

$$BH_3(OH)^- + 3\,H_2O = B(OH)_4^- + 3H_2 \quad [5]$$

Typical behaviour for gold in 1 mol dm^{-3} NaOH is seen in the cyclic voltammogram (CV) recorded over the potential range -0.75 to +0.68 V for a 10 μm diameter microdisc electrode shown in Fig 1. This voltammogram shows that negligible current (subnanoamp) flows in the absence of DMAB over the potential range -0.75 to -0.35 V. The onset of monolayer oxide formation is shown to occur above +0.05 V with the corresponding oxide reduction peak on the reverse sweep. This potential region leads to complications in the analysis of the second DMAB oxidation wave described below. When 10 mmol dm^{-3} DMAB is added to the 1 mol dm^{-3} NaOH solution a well-defined CV (Fig. 2) is achieved at a Au microdisc consisting of two irreversible anodic waves. The magnitude of the current for both anodic waves is equal. The first anodic wave commencing at –1.0 V exhibits a mass transport-controlled steady-state current at –0.55 V (see Fig. 3). A linear dependence of steady state current with concentration for the first wave was found over a restricted concentration range (5 to 130 mmol dm^{-3}) indicated in Fig. 4.

The second anodic wave commencing at –0.40 V is inhibited at 0.10 V due to Au monolayer oxide formation but is reactivated at 0.15 V in the subsequent reverse sweep as the oxide layer is reduced. Upon reduction of the oxide layer a new, catalytically active surface at the Au electrode forms thereby reactivating the surface

for DMAB oxidation. This results in an increase in the magnitude of the oxidation current for DMAB on the reverse sweep relative to the forward sweep. This type of behaviour has been observed for the oxidation of formaldehyde at a Ag-modified glassy carbon electrode [21] and for DMAB oxidation at Au macroelectrodes [8,17]. The complication of the coincident Au monolayer oxide formation in this potential region prohibits further analysis of this wave. The current achieved on the reverse sweep is two times that achieved for the first wave.

When the DMAB concentration exceeded 165 mmol dm^{-3} or alternatively when the ratio (R) of hydroxide ions to DMAB is below ca. 6 the measured currents did not increase linearly with DMAB concentration and the reverse sweep did not retrace the forward sweep. In these cases the evolution of gas, presumably hydrogen, was obvious. This result clearly indicates the upper useful concentration range for electroless plating baths in strongly alkaline solutions. This behaviour suggests the stoichiometry for the electrode reaction varies with R, realised as a decreased coulombic efficiency for DMAB oxidation when R is less than ca. 6 due to competing hydrogen evolution. Investigations by several groups into the oxidation of borohydride also revealed a variation of the coulomb number for borohydride oxidation with the ratio of borohydride to OH^- concentration [22-26].

The diffusion coefficient of DMAB was directly determined by analysing the chronoamperometric response for the first anodic wave which reaches a steady state at -0.55 V using a method introduced by Bard et al. [18] that does not require prior knowledge of n. They showed that the current ratio, $I_{(t)}/I_{ss}$, recorded for an electroactive species at a microdisc in response to a potential step is a linear function

of $t^{-1/2}$ and fits the expressions given in equations 6 and 7 for short and long current sampling times, respectively, following the potential step.

$$\frac{I(t)}{Iss} = 0.7854 + \left(\frac{\pi^{1/2}}{4}\right) r(Dt)^{-1/2} \qquad [6]$$

$$\frac{I(t)}{Iss} = 1 + \left(\frac{2}{\pi^{3/2}}\right) r(Dt)^{-1/2} \qquad [7]$$

where r is microdisc radius, I_{ss} is steady-state current and $I_{(t)}$ is current at time, t.

For 20 mmol dm^{-3} DMAB in 1 mol dm^{-3} NaOH an I_{ss} of 100 nA was recorded (conditions given in Figure 3 were employed). Current transients in response to a potential step from –1.15 to –0.55 V were recorded for this solution. The intercepts of the straight-line plots of $I_{(t)}/I_{ss}$ versus $t^{-1/2}$ shown in Figs. 5 and 6, for short and long times, respectively, suitably agree with those predicted theoretically. The D values determined from the slopes in Figs. 5 and 6 are comparable, with $D = 7.60\times10^{-6}$ cm^2 s^{-1} and 7.36×10^{-6} cm^2 s^{-1} for short and long times, respectively, giving an average value of 7.48×10^{-6} cm^2 s^{-1}.

Using the expression for the limiting current, I, under mass transport-controlled, steady state conditions at a microdisc electrode (equation 8) and 7.48×10^{-6} cm^2 s^{-1} for D, the coulomb number, n, was found to be 3.09.

$$I = 4nFDrC \qquad [8]$$

where r is microdisc radius and C is concentration of DMAB.

In their evaluation of peak current versus sweep rate ($\nu^{1/2}$) at a macroelectrode, Sargent et al. [7] estimated a value of 8.55×10^{-6} cm^2 s^{-1} for the diffusion coefficient of

DMAB where they assumed that 2 electrons were transferred in the oxidation reaction.

It may be tentatively assumed that D for the species responsible for the second anodic wave is comparable to that of the first. Hence, given that the oxidation current associated with the first and second stages is equal, a value of 3 for n has also been assigned to the second oxidation stage, implying a total 6-electron loss for DMAB oxidation. For low concentrations of DMAB (up to a maximum of 1 mmol dm^{-3}) the first anodic wave may be further resolved displaying three equal shoulders on the wave as shown in Fig.7. The transfer of 1 electron has been assigned to each step. The ability of microelectrodes to facilitate the analysis of low concentrations of electroactive species has enabled this identification of three 1-electron steps within the first oxidation wave which has not been reported previously for DMAB oxidation.

Osaka et al. [6] proposed the reaction mechanism given below with the exception of steps (b*), (d*) and (f*) to account for the overall oxidation reaction given earlier by equation 2. We propose a modified pathway replacing steps (b), (d) and (f) with (b*), (d*) and (f*), respectively, under conditions of sufficiently high OH^- content. Our pathway favours the OH^- ion-mediated electron removal over dehydrogenation for five-coordinate intermediate oxidation products, $BH_x(OH)_y^-$, where x + y = 5. A coulomb number of 6 estimated from the earlier data using the diffusion coefficient determined supports the electron transfer suggested in this modified scheme. The analysis of the first wave which showed a direct correlation between the wave height and DMAB concentration and the coulomb number of 3 for that reaction would also suggest that the proposed modified pathway is a realistic interpretation of the DMAB

oxidation mechanism. The hydrogen gas evolution pathway has been shown to be a limiting case in this mechanism when the ratio of constituents more readily facilitates this reaction. It is suggested that the 1-electron oxidation reactions shown in steps (a), (b*) and (c) may correspond to the three 1-electron oxidation steps observed in the cyclic voltammetric response shown in Fig. 7 for 0.90 mmol dm^{-3} DMAB at gold microdisc in 1 mol dm^{-3} NaOH at 100 mV s^{-1}.

Reaction pathway:

(a) $BH_3(OH)^- + OH^- = BH_3(OH)_2^- + e^-$

(b) $BH_3(OH)_2^- = BH_2(OH)_2^- + \frac{1}{2}H_2$

(b)* $BH_3(OH)_2^- + OH^- = BH_2(OH)_2^- + e^- + H_2O$

(c) $BH_2(OH)_2^- + OH^- = BH_2(OH)_3^- + e^-$

(d) $BH_2(OH)_3^- = BH(OH)_3^- + \frac{1}{2}H_2$

(d)* $BH_2(OH)_3^- + OH^- = BH(OH)_3^- + e^- + H_2O$

(e) $BH(OH)_3^- + OH^- = BH(OH)_4^- + e^-$

(f) $BH(OH)_4^- = B(OH)_4^- + \frac{1}{2}H_2$

(f)* $BH(OH)_4^- + OH^- = B(OH)_4^- + e^- + H_2O$

Combining steps (a)-(f*) with the omission of (b), (d) and (f) gives equation 4 where n is 6. Clearly to realise this n value and avoid hydrogen gas evolution R must equal or exceed 6. The reaction pathway proposed by Osaka et al. [6] including hydrogen gas evolution is a limiting case of the mechanism we propose which may be observed at low OH^- concentration. It is suggested that the actual oxidation of DMAB could

more realistically be described by equation 9, depending on the value of R, the ratio of OH^- to DMAB.

$$BH_3(OH)^- + nOH^- = B(OH)_4^- + (3-\frac{n}{2})H_2 + (n-3)H_2O + ne^- \quad [9]$$

where n = 3 - 6.

4. Conclusion

This work has shown that DMAB oxidation on gold microelectrodes may be observed to occur in two 3-electron waves. The first wave has been further resolved into three 1-electron steps. An overall coulomb number of 6 has been determined from the data acquired using the diffusion coefficient determined directly using chronoamperometry at the microdisc electrode. This analysis has yielded parameters that had not been previously established for this system. The concentration range over which the reproducible 6-electron oxidation was determined has been demonstrated. The stoichiometry of the reaction varies depending on the ratio of OH^- to DMAB, with hydrogen evolution gaining increasing significance as this ratio decreases. The oxidation can be more comprehensively described in terms of a variable coulomb number depending on the conditions employed. This result is potentially enabling in electroless deposition processing where the need for a better understanding of all aspects of the deposition process is key to the development and optimisation of electroless solutions.

Acknowledgements.

The authors thank the Irish Research Council for Science Engineering and Technology of Ireland (IRCSET) for financial support.

NMRC assisted in meeting the publication costs of this article.

References.

1. F. Pearlstein and RF.Weightman, *Plat*., **60,** 474 (1973).
2. M. Lelental, *J. Catal*., **32**, 429 (1974).
3. C.D. Iacovangelo, *J. Electrochem. Soc*., **138**, 976 (1991).
4. J.C. Patterson, C. Ni Dheasuna, J. Barrett, T.R. Spalding, M. O'Reilly, X.Jiang and G.M. Crean, *Appl. Surf. Sci.,* **91**, 124 (1995).
5. A. Chiba, H. Haijima and K. Kobayashi*, Surf. Coat. Tech.,* **169-170**, 104 (2003).
6. T. Homma, A. Tamaki, H. Nakai and T. Osaka, *J. Electroanal. Chem*., **559**, 131 (2003).
7. A. Sargent, O. Sadik and L. Matienzo, *J. Electrochem. Soc*., **148**, C257 (2001).
8. Y. Yamauchi, T. Yokoshima, H. Mukaibo, M. Tezuka, T. Shigeno, T. Momma, T. Osaka and K. Kuroda, *Chem. Lett*., **33,** 542 (2004).
9. T.Yokoshima, D.Kaneko, M.Makahori, H-S.Nam and T.Osaka, *J. Electroanal. Chem*., **491,** 197 (2000).
10. T.Yokoshima, S.Nakamura, D.Kaneko, T.Osaka, S.Takefusa and A.Tanaka, *J. Electrochem. Soc.,* **149,** C375 (2002).
11. T.Osaka, N.Takano, T.Kurokawa, T.Kaneko and K.Ueno, Su*rf. Coat. Tech*., **169–170**, 124 (2003).
12. T.S.N. Sankara Narayanan, A. Stephan and S. Guruskanthan, *Surf. Coat. Tech*., **179**, 56 (2004).
13. J.M.Izaki and T.Omi, *J. Electrochem.Soc*., **144**, L3 (1997).
14. M. Izaki and J.Katayama, *J. Electrochem. Soc.*, **147,** 210 (2000).

15. M.Chigane, M.Izaki, T.Shinagawa and M.Ishikawa, *Electrochem. Solid-State Lett.,* **7** D1 (2004).

16. E.J. O'Sullivan, *Advances in electrochemical science and engineering*, Volume 7, R.C.Alkire and D.M.Kolb Editors, p. 225 Wiley, New York, 2001.

17. L.D. Burke and B.H. Lee, *J. Appl. Electrochem*., **22,** 48 (1992).

18. G. Denault, M. Mirkin and A.J. Bard, *J. Electroanal. Chem*., **308**, 27 (1991).

19. M.V. Mirkin, H.Yang and A.J. Bard, *J. Electrochem. Soc.*, **139,** 2212 (1992).

20. A.D'Ulivo, Spectrochim. Acta, B, **59**, 798 (2004).

21. M. Avramov-Ivic, V. Jovanovic, G. Vlanjnic and J. Popic, *J. Electroanal. Chem*., **423** 119 (1997).

22. J.A. Gardiner and J.W. Collat, *J. Am. Chem. Soc*., **87**, 1692 (1965).

23. J.A. Gardiner and J.W. Collat, *Inorg. Chem*., **4**, 1208 (1965).

24. S. Amendola, P. Onnerud, M. Kelly, P. Petillo, S. Sharp-Goldman and M. Binder, *J. Power Sources,* **84**, 130 (1999).

25. E. Gyenge, *Electrochim. Acta,* **49**, 965 (2004).

26. B. Hong Liu, Z. Peng Li and S. Suda, *Electrochim. Acta*, **49**, 3097 (2004).

Figure legends.

Fig.1 Cyclic voltammogram (-0.75 to +0.68 V) at gold microdisc in 1 mol dm^{-3} NaOH at 100 mV s^{-1}.

Fig.2 Cyclic voltammogram (-1.15 to 0.50 V) of 10 mmol dm^{-3} DMAB at gold microdisc in 1 mol dm^{-3} NaOH at 100 mV s^{-1}.

Fig. 3. Cyclic voltammogram (-1.15 to -0.55 V) of DMAB (a) 5, (b) 40, (c) 70 and (d) 130 mmol dm^{-3} at gold microdisc in 1 mol dm^{-3} NaOH at 100 mV s^{-1}.

Fig. 4 Plot of steady-state current at –0.55 V vs. concentration for 10 mmol dm^{-3} DMAB at gold microdisc in 1 mol dm^{-3} NaOH at 100 mV s^{-1}.

Fig. 5 Plot of ratio of $I_{(t)}/I_{ss}$ vs. inverse $t^{-1/2}$ for 20 mmol dm^{-3} DMAB at gold microdisc in 1 mol dm^{-3} NaOH. $I_{(t)}$ in response to a potential step from –1.15 to –0.55 V was recorded at a sampling rate of 0.1 ms per point over a timescale of 0.9 s.

Fig. 6 Plot of ratio of $I_{(t)}/I_{ss}$ vs. inverse $t^{-1/2}$ for 20 mmol dm^{-3} DMAB at gold microdisc in 1 mol dm^{-3} NaOH. $I_{(t)}$ in response to a potential step from –1.15 to –0.55 V was recorded at a sampling rate of 10 ms per point over a timescale of 9 s.

Fig. 7 Cyclic voltammogram (-1.15 to -0.55 V) of 0.90 mmol dm^{-3} DMAB at gold microdisc in 1 mol dm^{-3} NaOH at 100 mV s^{-1}.

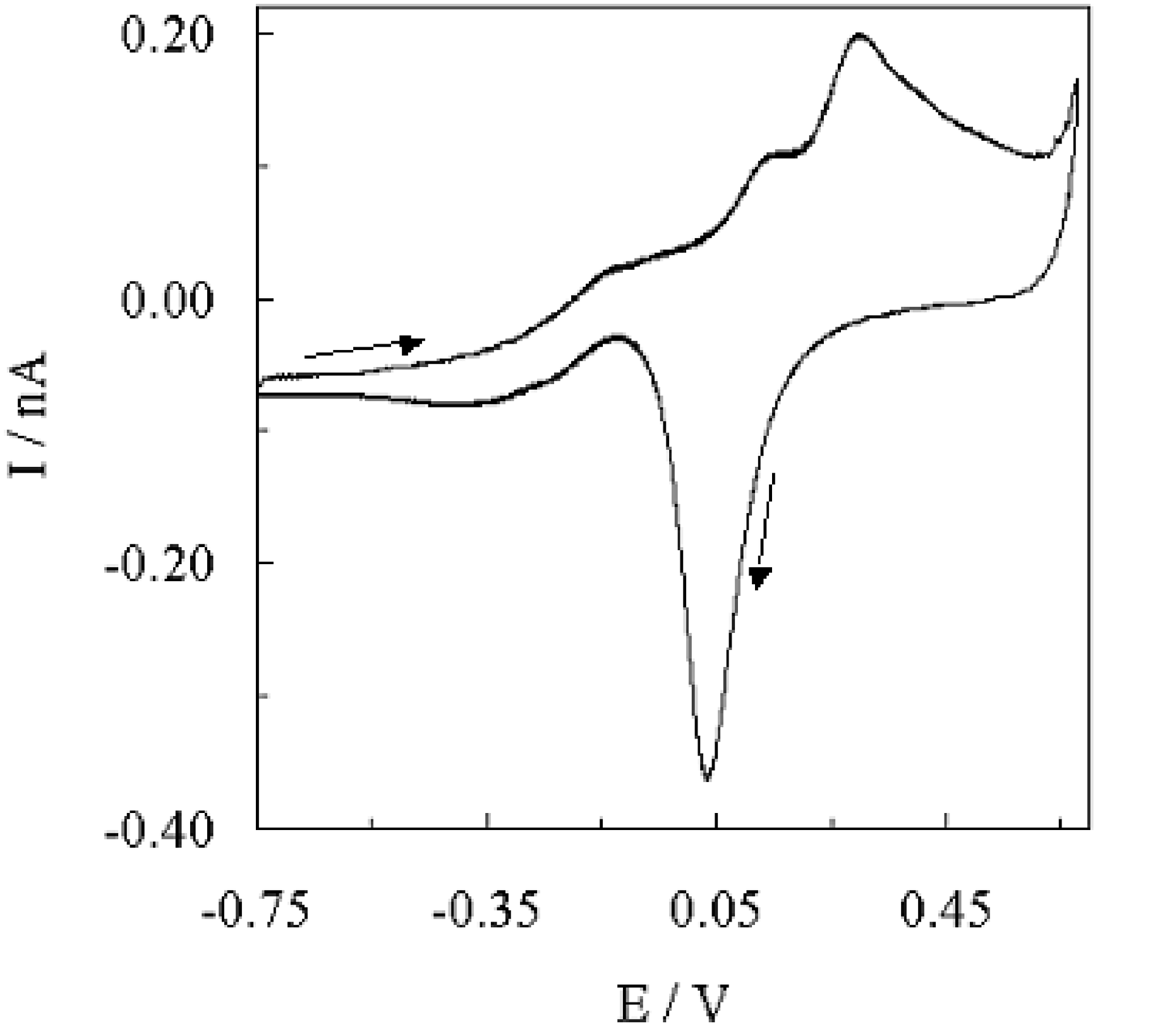
0.20
0.00
-0.20
-0.40
I / nA
-0.75
-0.35
0.05
0.45
E / V

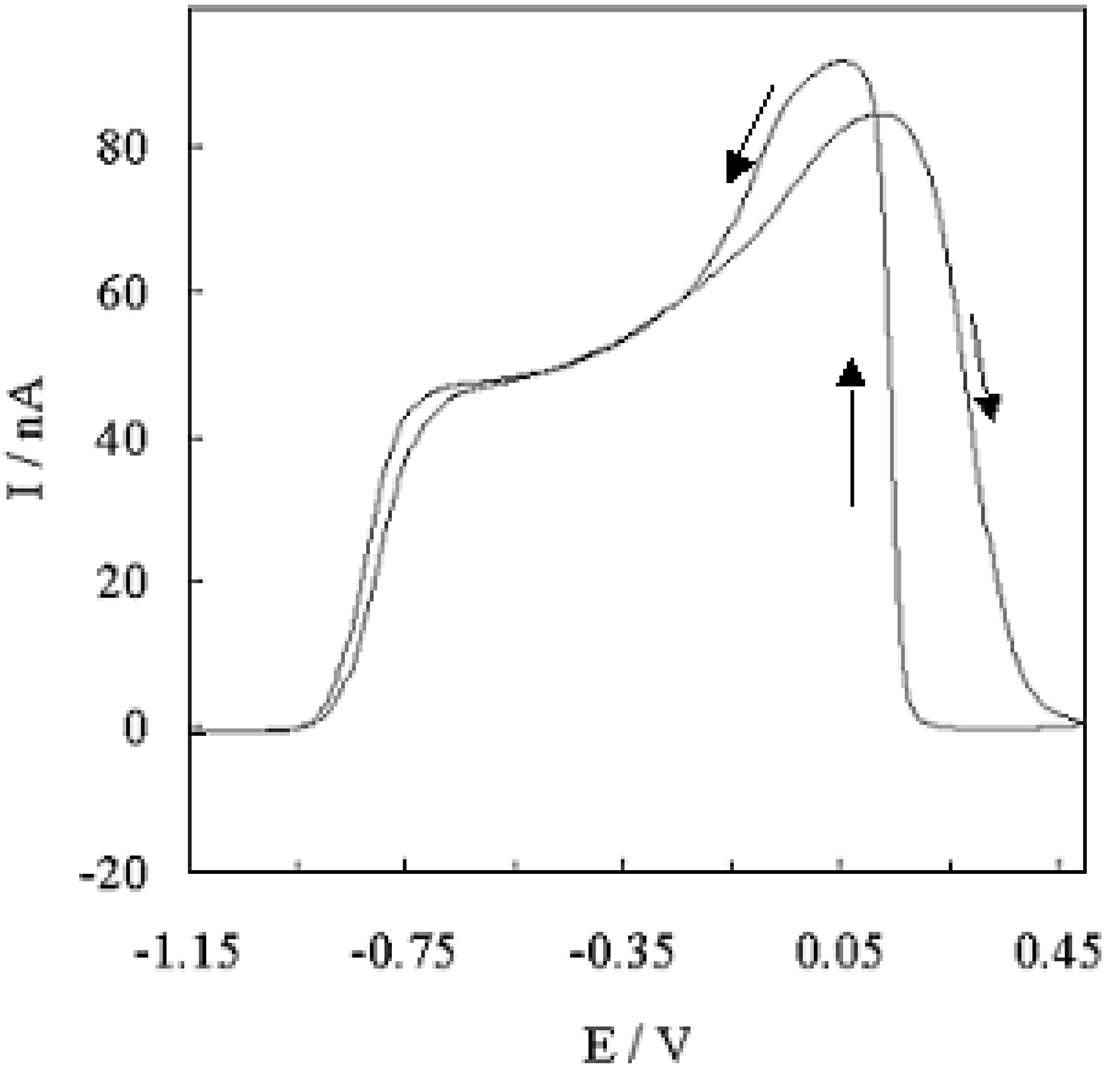
80
60
40
20
0
-20
I / nA
-1.15
-0.75
-0.35
0.05
0.45
E / V

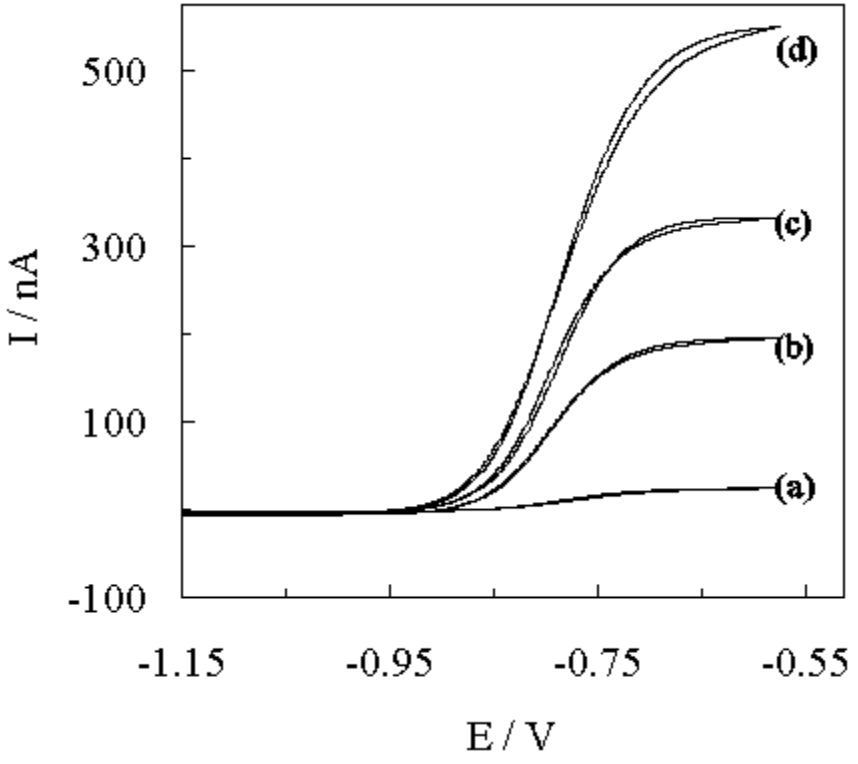
500
300
100
-100
I / nA
-1.15
-0.95
-0.75
-0.55
E / V
(a)
(b)
(c)
(d)

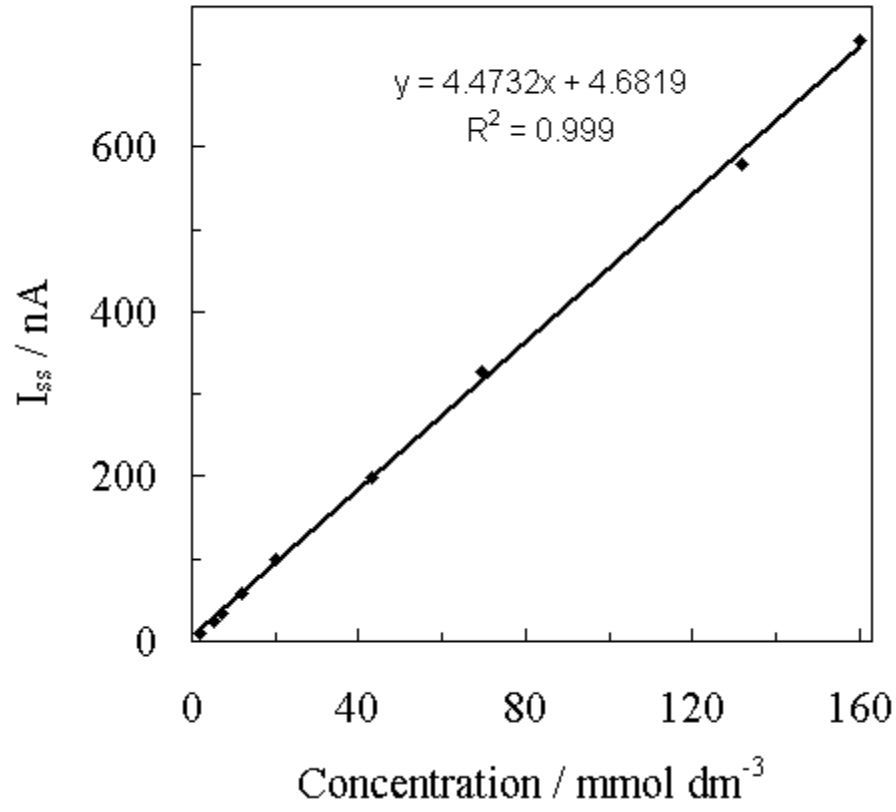
y = 4.4732x + 4.6819
R2 = 0.999
600
400
200
0
Iss / nA
0
40
80
120
160
Concentration / mmol dm-3

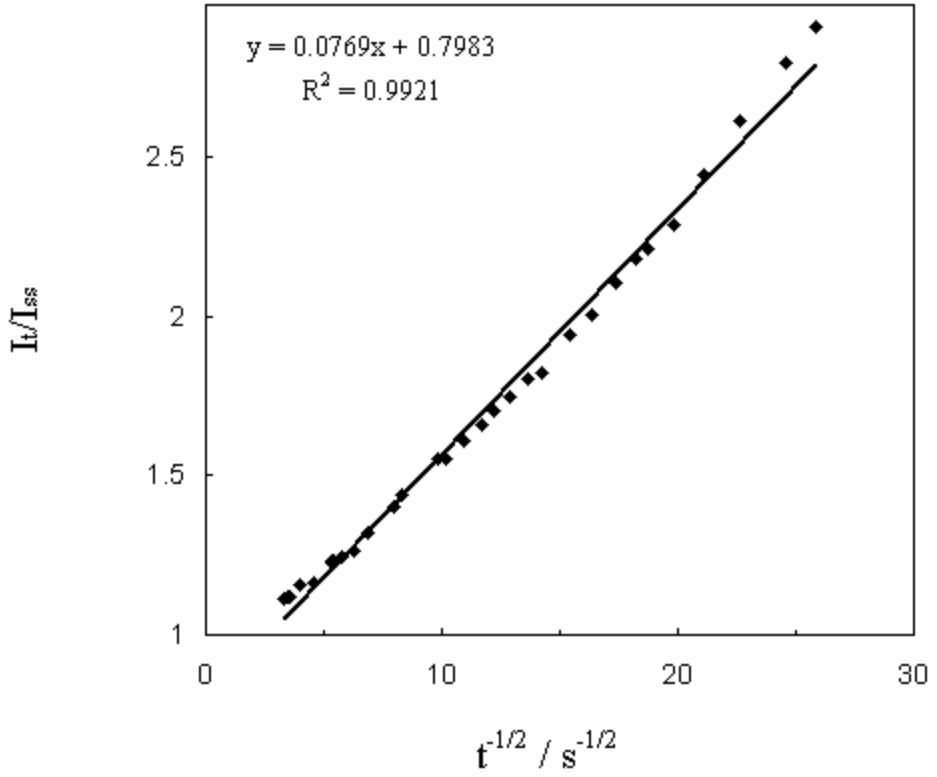
y = 0.0769x + 0.7983
R2 = 0.9921
2.5
2
1.5
1
0
10
20
30
It/Iss
t-1/2 / s-1/2

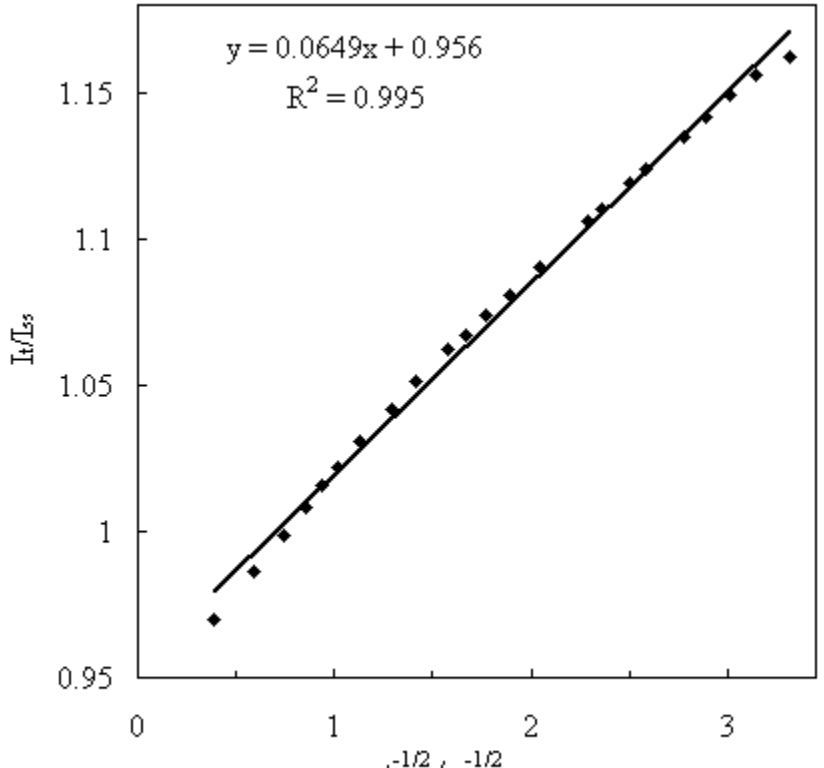
y = 0.0649x + 0.956
R2 = 0.995
1.15
1.1
1.05
1
0.95
It/Is
0
1
2
3
t-1/2 / s-1/2

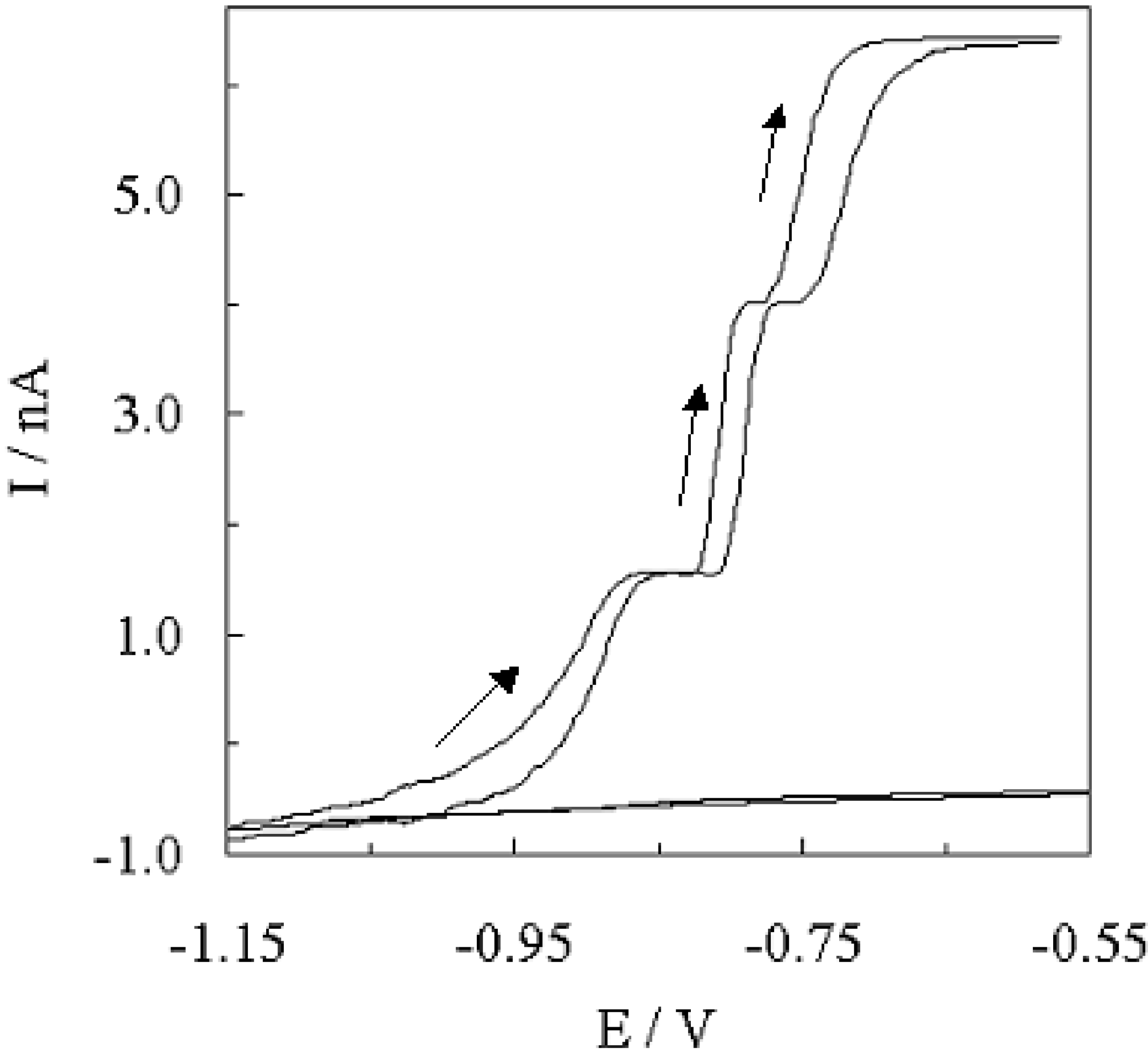
5.0
3.0
1.0
-1.0
I / nA
-1.15
-0.95
-0.75
-0.55
E / V